ACS APPLIED NANO MATERIALS

www.acsanm.org Article

Cerium Oxide Nanoparticle-Containing Colorimetric Contact Lenses for Noninvasively Monitoring Human Tear Glucose

Sijin Park, Juil Hwang, Hee-Jae Jeon, Woo Ri Bae, In-Kyung Jeong, Tae Gi Kim, Jaheon Kang, Young-Geun Han, Euiheon Chung, and Dong Yun Lee*

Cite This: *ACS Appl. Nano Mater.* 2021, 4, 5198−5210 Read Online

ACCESS | Metrics & More | Article Recommendations | Supporting Information

ABSTRACT: Noninvasive methods for monitoring diabetes are being developed to eliminate the need for invasive finger-prick testing. Here, we propose the noninvasive detection of tear glucose using contact lenses that contain cerium oxide nanoparticles (CNPs). We chemically conjugated CNPs with glucose oxidase (GOx) using poly(ethylene glycol) (PEG) (CNP-PEG-GOx). GOx oxidizes glucose into hydrogen peroxide, which rapidly (~1 min) reduces colorless Ce^{3+} to yellow Ce^{4+} with high sensitivity (>0.1 mM). Then, the yellow CNP-PEG-GOx can be analyzed to quantify the glucose concentration using a smartphone equipped with an image-processing algorithm. The CNP-PEG-GOx-laden contact lenses had physical properties similar to those of commercially available contact lenses and were nontoxic to human corneal cells and endothelial cells. When the CNP-PEG-GOx-laden contact lenses were placed on the eyes of diabetic rabbits, it was possible to measure the tear glucose levels. Interestingly, the lenses successfully detected glucose in human tear specimens and distinguished the diabetes status of patients. These findings suggest that the CNP-PEG-GOx-laden contact lenses could be used along with a smartphone-based image-processing algorithm to noninvasively monitor human tear glucose.

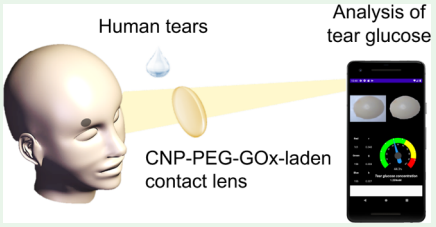

KEYWORDS: *cerium oxide nanoparticles, glucose, diabetes, tear glucose sensing, smartphone*

1. INTRODUCTION

The incidence of diabetes, a chronic disease among the top 10 causes of death, is increasing dramatically around the world.[1,2] The chronically raised blood glucose found in diabetes patients is a major risk factor for microvascular complications such as stroke and peripheral vascular disease.[3−5] To manage blood glucose and complications, the standard for diabetes care is the delivery of insulin and self-monitoring of blood glucose, which is necessary not only to determine the timing for insulin injections but also to monitor for hypoglycemia or hyperglycemia after insulin administration. Currently, glucose self-monitoring is performed using a finger-prick test with a portable reading device, which is a nearly complete method. However, the pain of the finger-prick severely reduces patient compliance with frequent glucose monitoring.[6,7] Therefore, a minimally invasive strategy for glucose self-monitoring is needed. To that end, studies are being conducted to detect glucose in extracorporeal body fluids such as urine, saliva, sweat, and tears.[8]

Measuring glucose levels in tears using contact lenses might be the most ideal method because contact lenses have been the most popular wearable medical device for many years. In other words, patients with vision problems already wear contact lenses independently, and they show no serious side effects, even when worn for a long time. Therefore, many lens-based emerging technologies are being developed, such as electrochemical, photonic crystal, and fluorescence-based contact lenses. Electrochemical contact lenses require power to run their on-chip systems and wireless circuits,[9−15] but they have a rapid readout time (<100 s) and high glucose sensitivity (0−5 mM).[10,16,17] Representatively, Google and Novartis developed the Google lens to diagnose diabetes and glaucoma.[9] On the other hand, fluorescence-based[18,19] and photonic crystal-based[20−22] contact lenses have longer readout times (<30 min) but detect a broader range of glucose concentrations (0−50 mM) and do not require a power source. All of the emerging "smart" contact lenses still face challenges, such as reliability, safety, toxicity, and manufacturing cost, before they will be ready for clinical applications. Therefore, other advances in smart contact lenses are focused on making them simpler, cheaper, and faster.

In this research, we suggest a colorimetric contact lens, which is attractive because colorimetric biosensors generally enable simple, practical, and cheap detection of target molecules without requiring any sophisticated instrumentation. To transform the detection of tear glucose into color changes in a colorimetric contact lens, we use cerium oxide nano-

Received: March 2, 2021
Accepted: May 5, 2021
Published: May 17, 2021

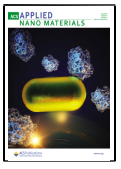

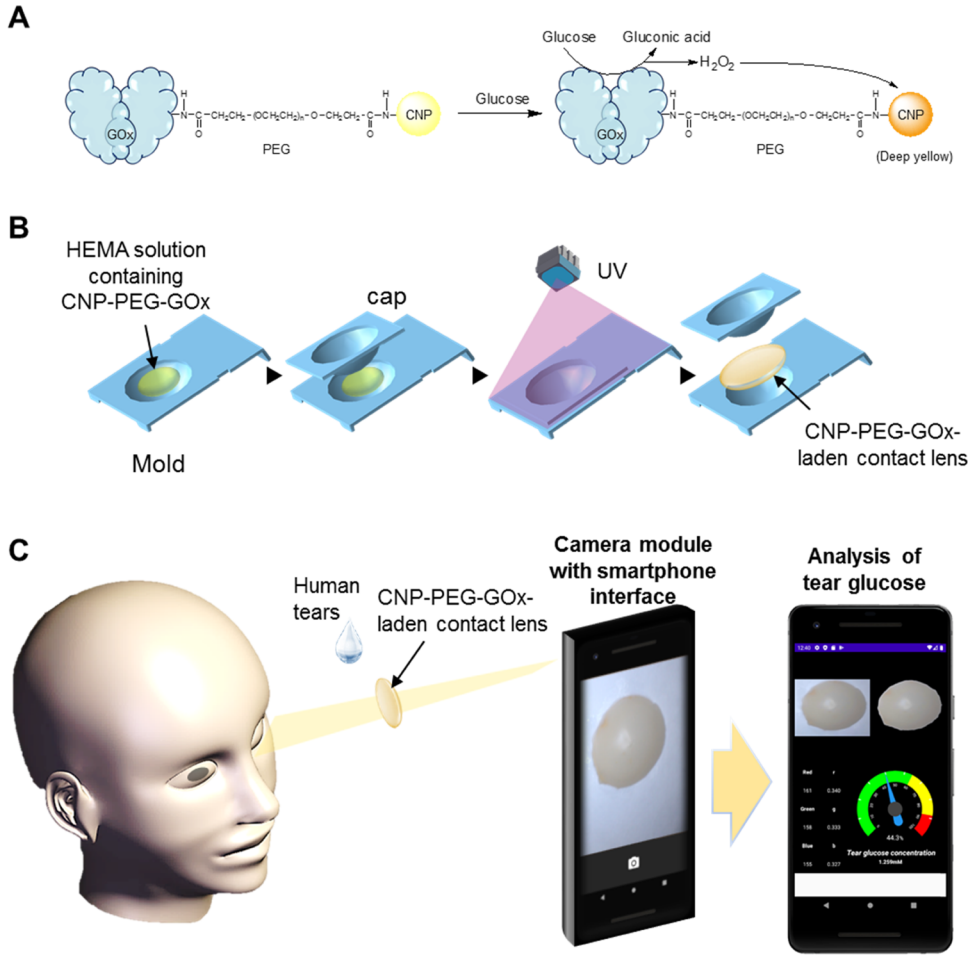

Figure 1. Schematic illustration of the colorimetric contact lens-based glucose monitoring platform. (A) Schematic illustration of the mechanism for yellow color generation by CNP-PEG-GOx. (B) Schematic of the fabrication process for a CNP-PEG-GOx-laden contact lens from a general contact lens mold using photopolymerization. (C) RGB color analysis using the smartphone-based image-processing algorithm.

particles (CNPs) as the "signal transducer." CNPs have recently been recognized as "nanozymes" due to their enzyme-like activity,[23−25] which stems from the two oxidation states of cerium, i.e., Ce^{3+} and Ce^{4+}, which produce oxygen vacancies at the nanoparticle surface. Interestingly, the oxidation of surface-exposed Ce^{3+} into Ce^{4+} at the nanoparticle surface can produce unique color changes in the nanoparticle (Figure 1A) without causing any problems of enzyme instability.[26−28] In fact, enzyme-like CNPs have been widely investigated for their potential development as robust and reliable immunoassays and biosensors.[29−31] Based on these findings, CNPs can be used with glucose oxidase to detect glucose molecules.[32−34] Glucose oxidase (GOx) generally catalyzes the oxidation of glucose into H_2O_2 and D-glucono-δ-lactone. Therefore, to make colorimetric contact lenses, CNPs were chemically conjugated with GOx through a link with biocompatible poly(ethylene glycol) (PEG), and that combination was called the CNP-PEG-GOx nanocomplex (Figure 1A). CNP-PEG-GOx nanocomplexes were mixed with (hydroxyethyl)-methacrylate (HEMA) solution and polymerized (Figure 1B). To quantify the intensity of color changes in the CNP-PEG-GOx-infused colorimetric contact lenses, we propose a smartphone-based image-processing algorithm. Using a smartphone for scientific imaging has several advantages, such as not requiring additional electricity and a camera module with sufficient color and image resolution. In practice, smartphones are already being used in chemical and biological applications for medical diagnostics.[35−39] Therefore, to directly quantify colorimetric detection in the smartphone interface, we built a correction algorithm that can measure the color change of the colorimetric contact lens with the same accuracy as a benchtop spectrometer (Figure 1C). In this study, we demonstrate that our wearable CNP-PEG-GOx-laden contact lenses can be used with our smartphone-based image-processing algorithm to monitor tear glucose levels in diabetic rabbits. We also used human tear specimens to confirm the ability of this new platform to distinguish the diabetes status of patients.

2. RESULTS AND DISCUSSION

2.1. Characterization of CNP-PEG-GOx. CNPs were chemically prepared using a method modified from a previous report.[40] The size of the synthesized CNPs was ~6 nm in diameter (Figure 2A,B). In an X-ray photoelectron spectroscopy (XPS) analysis, we confirmed that our CNPs had a specific lattice structure of oxygen (~37.8%) and cerium (~62.2%) atoms (Figure S1a,b). We then analyzed the development of yellow in the CNPs according to the concentration of H_2O_2 or glucose using GOx. The relationship between the analyte levels and color was confirmed using a normalized *b* color profile algorithm that gives a chromaticity diagram as a complementary color of yellow (Figure S2). The

https://doi.org/10.1021/acsanm.1c00603
ACS Appl. Nano Mater. 2021, 4, 5198−5210

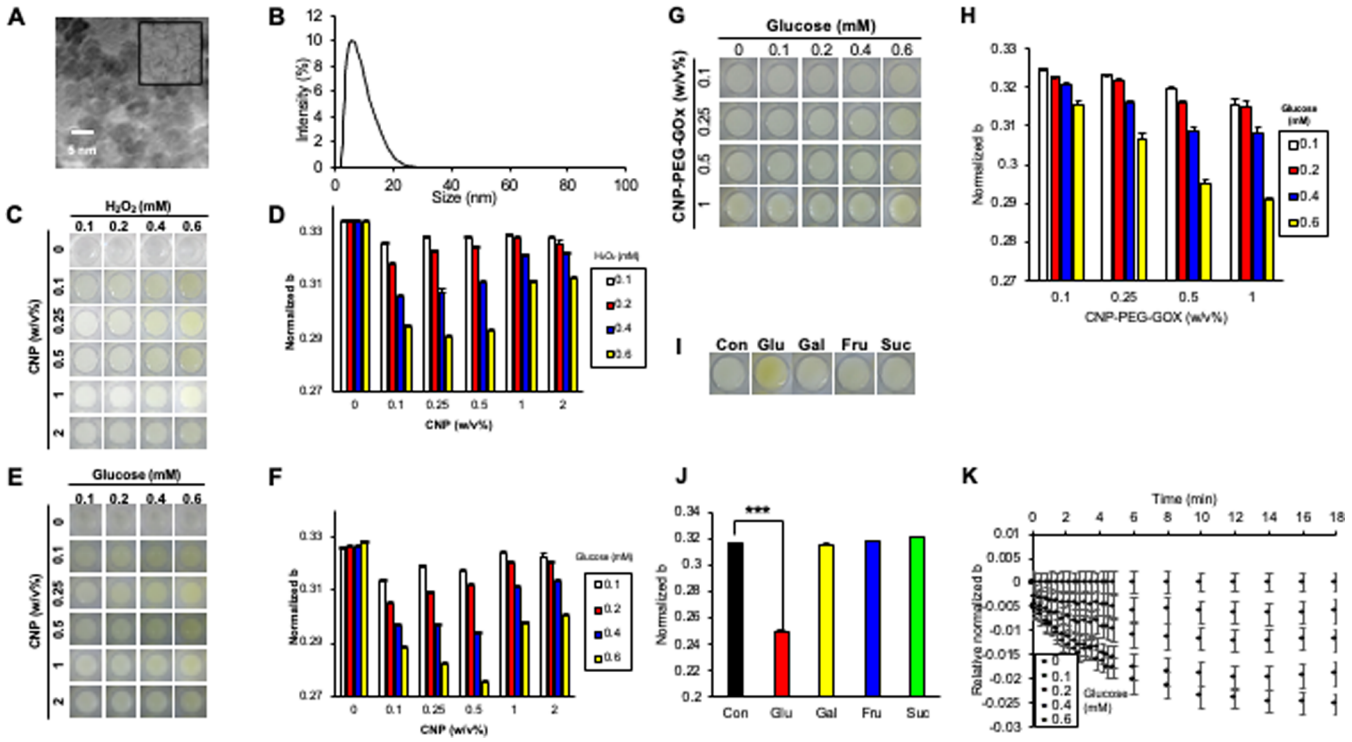

Figure 2. Characterization of the CNPs and CNP-PEG-GOx. (A) High-resolution transmission electron microscopy (HR-TEM) image of CNPs showing the distinct structure of the nanoparticles (magnification = ×500 000. Scale bar = 5 nm). Inset: HR-TEM image of CNPs (magnification = ×100 000. Scale bar = 20 nm). (B) Dynamic light scattering (DLS) data for the CNPs. The size of the CNPs was ~6.5 nm. (C) Color development of various concentrations of CNPs upon exposure to various concentrations of hydrogen peroxide (H_2O_2) for 2 min and (D) the normalized *b* color profile analysis. Data are presented as the mean ± standard error of the mean (SEM) (n = 5). (E) Color development of various concentrations of CNPs in the presence of glucose oxidase (GOx; 100 U/mL) and various concentrations of glucose for 2 min and (F) the normalized *b* color profile analysis. Data are presented as the mean ± SEM (n = 5). (G) Color development of various concentrations of CNP-PEG-GOx at various concentrations of glucose for 2 min and the normalized *b* color profile analysis. Data are presented as the mean ± SEM (n = 5). (I) Selectivity of CNP-PEG-GOx (1 w/v%) against 5 mM glucose (Glu), fructose (Fru), galactose (Gal), and sucrose (Suc) for 2 min and (J) the normalized *b* color profile analysis. Data are presented as the mean ± SEM (n = 5). ***P < 0.001. (K) Time-dependent responsiveness of CNP-PEG-GOx (1 w/v%) after treatment with various concentrations of glucose, which was analyzed as the normalized *b* color profile. Data are presented as the mean ± SEM (n = 5).

color of the CNP solution immediately and dose-dependently became yellow upon exposure to different concentrations of H_2O_2 (Figure 2C,D) and glucose (Figure 2E,F) in the presence of GOx (100 U/mL). However, when the concentration of CNPs exceeded 0.5% (w/v), the R_2 value of the linear regression graph decreased to less than 0.99 because of the background color of the solution when a high number of CNPs was present (Figures S3 and S4). Based on these findings, we confirmed that the synthesized CNPs dose-dependently became yellow in the presence of directly administered or enzymatically generated H_2O_2.

To synthesize the CNP-PEG-GOx conjugate, we introduced a functional amine group onto the CNP surfaces via the ring opening of epichlorohydrin (CNP-NH_2) and then chemically conjugated *N*-hydroxysuccinimide (NHS)-functionalized polyethylene glycol (PEG-NHS, 2 kDa) to CNP-NH_2 via an amide linkage (CNP-PEG) (Figure S5). The chemical modification of CNP with PEG was confirmed by XPS and Fourier transform infrared (FT-IR) analyses (Figure S6). Then, carboxyl groups of CNP-PEG were chemically conjugated with GOx through NHS and 1-ethyl-3-(3-dimethylaminopropyl)carbodiimide (EDC) chemistry (Figure S7). The CNP-PEG-GOx conjugate was confirmed by UV−vis absorbance spectra (Figure S8). The peaks of GOx and CNP in CNP-PEG-GOx were detected at 255 and 280 nm, respectively. When CNP-PEG (as prepared, with a 1:0.25 feed ratio) was reacted with GOx, the amount of conjugated GOx was 464.5 ± 15.9 μg per 1 mg of CNP-PEG-GOx (Table S1). However, when a longer length of PEG (5 kDa) was used, the GOx did not sufficiently conjugate to CNP-PEG, possibly because of the higher mobility of PEG.[41,42] The chemical conjugation of GOx to CNP-PEG was confirmed by sodium dodecyl sulfate-polyacrylamide gel electrophoresis (SDS-PAGE) (Figure S9). The detection of the GOx band in CNP-PEG-GOx using free GOx (lane #4) suggests that CNP-PEG-GOx itself did not affect the mobility of GOx in the gel. In other words, finding no band of GOx in CNP-PEG-GOx (lane #3) indicated that GOx was not physically attached to the CNPs. The sensing characteristics of CNP-PEG-GOx were determined using a low concentration of glucose analyte (Figure 2G−K). CNP-PEG-GOx specifically and dose-dependently recognized the glucose analyte at each concentration of CNP-PEG-GOx (Figure S10). In addition, it responded to the glucose analyte within 1 min, and in around 10 min, its color development became saturated. In the clinic, human tears vary depending on the method of collection, but they usually have low glucose levels (0.1−10 mg/dL).[43] Therefore, our CNP-PEG-GOx could monitor tear glucose due to its high sensitivity, selectivity, and rapid responsiveness.

https://doi.org/10.1021/acsanm.1c00603
ACS Appl. Nano Mater. 2021, 4, 5198−5210

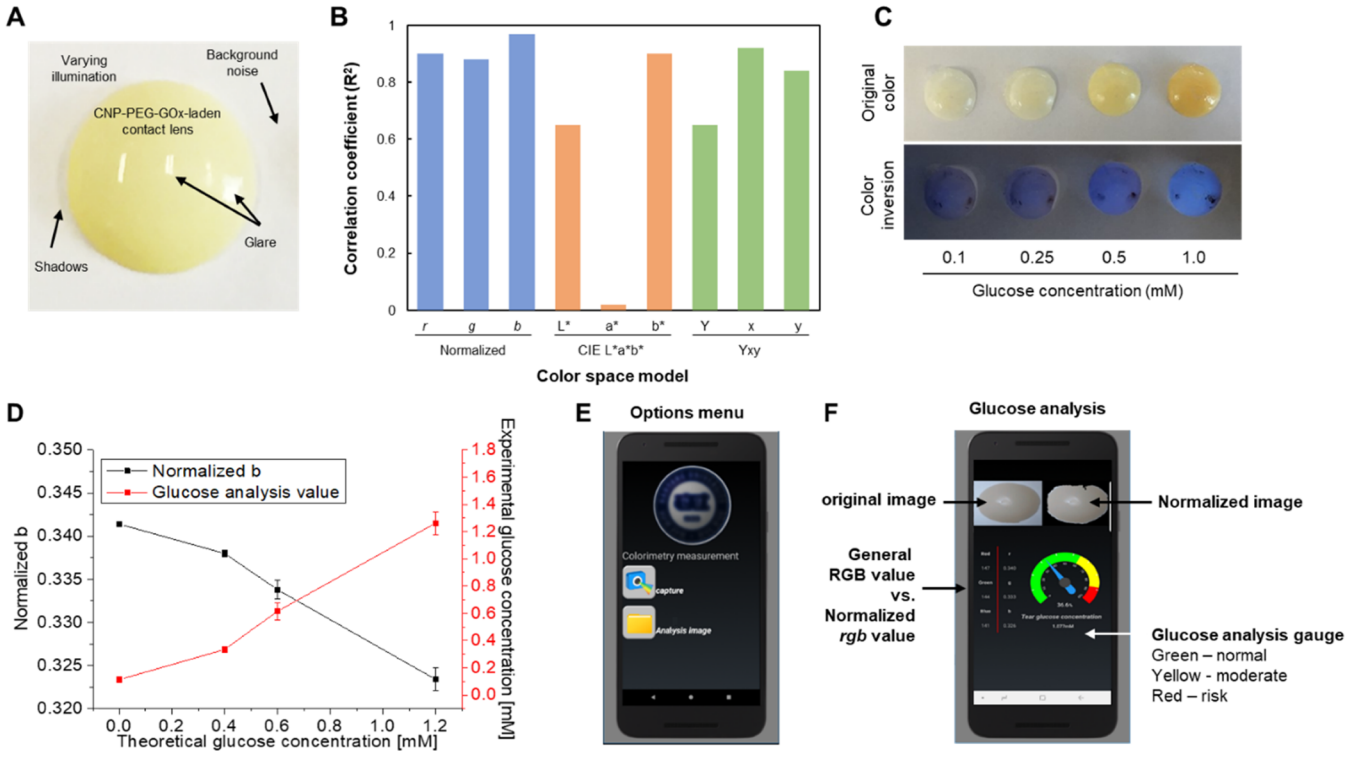

Figure 3. Smartphone-based algorithm interface for monitoring colorimetric contact lenses. (A) Inhomogeneous illumination-based noise generation, such as background noise, varying illumination, shadows, and glare on the contact lenses. (B) Correlation coefficient (R^2) determined through a regression analysis on the color change in different color space models. (C) Relationship between the developed color of the lens and the complementary color with different concentrations of glucose. (D) Relationship between the normalized *b* color profile and the real glucose concentration in vitro. (E) Starting interface for the glucose colorimetric detection app with an options menu. (F) Photograph of original/normalized color images with the original RGB/normalized *rgb* color profiles and the value of tear glucose concentration calculated in the app.

2.2. Smartphone-Based Algorithm Interface for Monitoring Colorimetric Contact Lenses. The optical colorimetric measurement technique was used to monitor the development of a yellow color on the CNP-PEG-GOx-laden contact lenses. When a contact lens is illuminated by a conventional digital camera under both directional and inhomogeneous illumination, different noises, such as background noise, varying illumination, shadows, and glare, are inevitably induced in the optical images by the curved shape of the lens itself[44−46] (Figure 3A). These noises can severely degrade the colorimetric information. To mitigate this noise, therefore, a smartphone-based algorithm interface was coded for the quantitative analysis of glucose (Figure S11). After eliminating the shadow and background noise outside of the lens, a three-dimensional (3D) RGB color profile in the spatial domain was obtained for the lens using the mask image procedure, and it was converted to the planar two-dimensional (2D) normalized *rgb* color profile in the spatial domain through intensity normalization and an image reconstruction procedure (Figure S12). In the color value detection step, each average value of the normalized *rgb* color profile was calculated and used to determine the quantitative concentration of glucose in the corresponding standard reference. After that, we compared several color space models to determine which color factor in the various color profiles best reflected the change in glucose concentration. Representative color spaces, i.e., CIE *L*a*b** and CIE *Yxy*, were compared with our normalized *rgb* model (Figure 3B). The correlation coefficient (R^2) was obtained for each color space model using a regression analysis of the color changes with different concentrations of glucose. The R^2 value indicates the covariance of the variable divided by the product of the standard deviation.[47,48] The sensitivity to a blue color change at the normalized *b* (blue bar; R^2 = 0.97) was very high. Also, the change in the blue color profile, a complementary color of yellow/orange, was high through color inversion (Figure 3C). In fact, the glucose concentration (red line) and each normalized *b* color profile (black line) appeared in a strong inverse proportion to each other (Figure 3D). Therefore, the glucose concentration was predicted by measuring the normalized *b* color profile as the analytic color factor. This algorithm interface was ported to the Android OS using Android Developer Tools in Java and OpenCV in C^{++} (Figure 3E,F). The smartphone app shows the measured average RGB color profile, normalized *rgb* color profile, and calculated glucose concentration on its analysis gauge after importing captured or prerecorded contact lens images. Therefore, users could easily access their own glucose monitoring and diabetic risk through this gauge. For the operating tests, the app was installed on a Samsung Galaxy S9^{+} device running Android version 8.0.0. (Figure S13 and Movie S1).

2.3. Characterization of the CNP-PEG-GOx-Laden Contact Lenses. Contact lenses must be comfortable because they are applied directly to the naked eye. Therefore, to evaluate the wearability of the CNP-PEG-GOx-laden contact lenses, their physical properties were compared with those of a commercially available soft lens made of the (hydroxyethyl)-methacrylate (HEMA) polymer. The light transparency of the lens was gradually attenuated as the CNP-PEG-GOx content increased (Figure 4A,B). However, the elastic modulus value

https://doi.org/10.1021/acsanm.1c00603
ACS Appl. Nano Mater. 2021, 4, 5198−5210

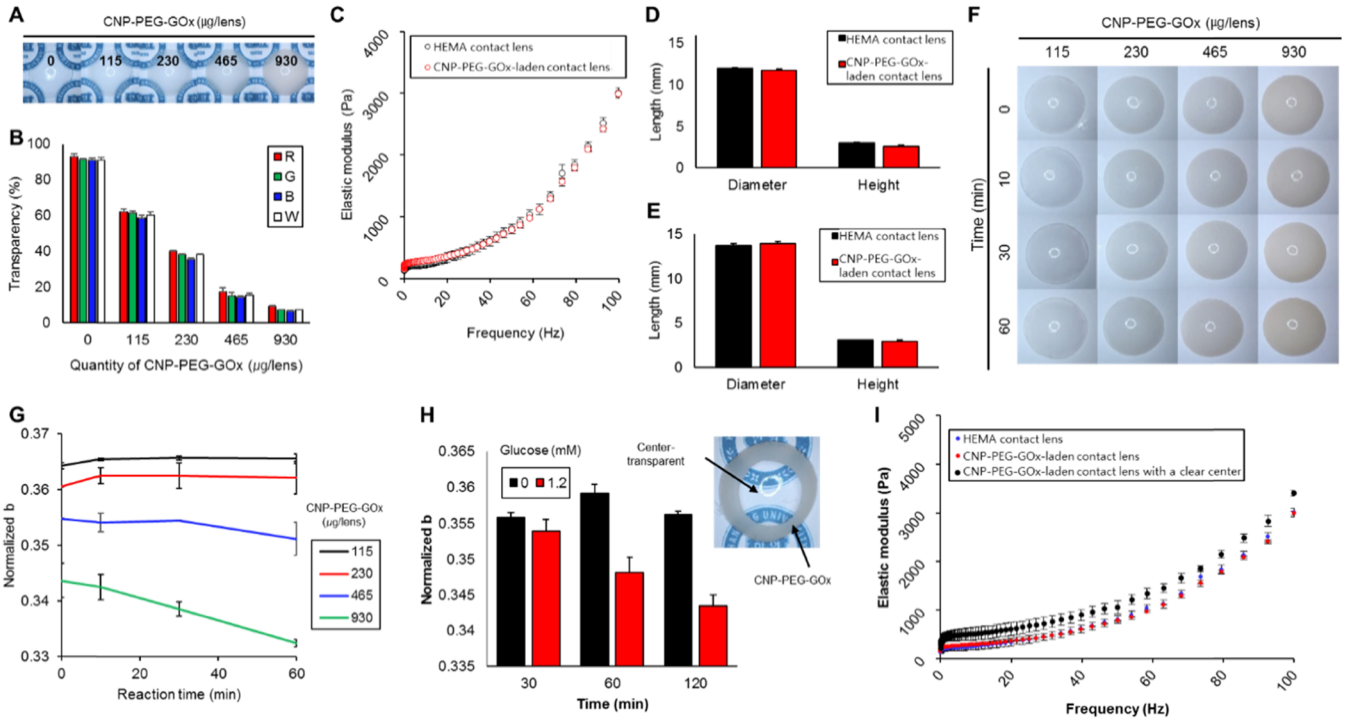

Figure 4. Characterization of CNP-PEG-GOx-laden contact lenses. (A) Photograph of the CNP-PEG-GOx-laden contact lenses containing various amounts (0, 115, 230, 465, and 930 μg/lens) of CNP-PEG-GOx. (B) Measurement of RGBW light transparency (%) of each lens according to the amount of CNP-PEG-GOx. Data are presented as the mean ± SEM (n = 3). (C) Elastic modulus of the CNP-PEG-GOx-laden contact lenses (930 μg/lens) and HEMA contact lenses without CNP-PEG-GOx (control group). Data are presented as the mean ± SEM (n = 3). (D) Diameter and height of the CNP-PEG-GOx-laden contact lenses (930 μg/lens) and HEMA contact lenses without CNP-PEG-GOx (control group) before hydration. Data are presented as the mean ± SEM (n = 3). (E) Diameter and height of the CNP-PEG-GOx-laden contact lenses (930 μg/lens) and HEMA contact lenses without CNP-PEG-GOx (control group) after hydration. Data are presented as the mean ± SEM (n = 3). (F) Color image of the CNP-PEG-GOx-laden contact lenses according to the amount of CNP-PEG-GOx (115, 230, 465, and 930 μg/lens) after reaction with glucose (0.6 mM) for different reaction times (0, 10, 30, and 60 min). (G) Normalized b color profile of the CNP-PEG-GOX-laden contact lenses according to the amount of CNP-PEG-GOx (115, 230, 465, and 930 μg/lens) after reaction with glucose for different reaction times (0, 10, 30, and 60 min). Data are presented as the mean ± SEM (n = 5). (H) Normalized b color profile of the center-transparent contact lenses with CNP-PEG-GOx (930 μg/lens) (inset photograph) after treatment with glucose (1.2 mM). Data are presented as the mean ± S.EM (n = 3). (I) Elastic modulus of the CNP-PEG-GOx-laden contact lenses (930 μg/lens), center-transparent contact lenses with CNP-PEG-GOx, and HEMA contact lenses without CNP-PEG-GOx (control group). Data are presented as the mean ± SEM (n = 3).

was very similar to that of the HEMA contact lens even when the CNP-PEG-GOx loading was high (930 μg/lens) (Figure 4C). In addition, the results before and after hydration of the lens did not differ significantly (38−40%) in the equilibrium water content (EWC) between the two types of lenses, suggesting that the loaded CNP-PEG-GOx did not affect the swelling of the hydrogel lens (Figure 4D,E). The structural stability of the CNP-PEG-GOx-laden lens was analyzed using an electron microscope (Figure S14). The surface and cross-sectional images of the CNP-PEG-GOx-laden lens were smoother than those of the lens loaded with a mixture of CNP and GOx (no conjugation between them), perhaps because of leaks of the free GOx. In fact, almost all of the GOx leaked from the lenses loaded with a mixture of CNP and GOx, whereas no GOx was detected (ND) in the CNP-PEG-GOx-laden contact lenses (Figure S15). Therefore, the normalized b color profile of the two types of contact lenses differed significantly due to the leakage of the free GOx enzyme (Figure S16). These findings suggest that the PEG chemical link between the CNPs and GOx is important to enhance the structural stability of the CNP-PEG-GOx-laden contact lenses. In addition, the PEG linker (length ∼ 32 nm) might precisely maintain the distance between the CNPs and GOx, thereby facilitating the rapid reaction of H_2O_2 from the GOx.

To optimize the concentration of CNP-PEG-GOx in the contact lenses to accurately detect low concentrations of tear glucose, 0.6 mM glucose, which is observed in typical diabetes patients, was reacted with the lenses for different reaction times (Figure 4F,G).[49] When 930 μg of CNP-PEG-GOX was loaded onto contact lenses, yellow color development occurred on the entire surface of the lenses within 30 min, and CNP-PEG-GOx saturation occurred within 5 min (Figure 2F). The CNP-PEG-GOx-laden contact lenses required at least 30 min because the nanoparticles were trapped in the hydrogel. In addition, because the slope value of the plot for the normalized b color profile over time was obtained, the lenses should be able to detect low concentrations of tear glucose well. In fact, the CNP-PEG-GOx-laden contact lenses with 930 μg/lens showed very high reliability at even very low glucose concentrations (Figure S17). Furthermore, the normalized b color profile of the CNP-PEG-GOx-laden contact lenses was the same in buffer and artificial tears, suggesting that it could react to glucose in tears and develop color when worn on the eyes of healthy or diabetic patients (Figure S18). When glucose is catalyzed by GOx, glucuronic acid is produced as a byproduct, and it can affect the enzymatic reaction via pH change. Therefore, the color development of the CNP-PEG-GOx-laden contact lenses and pH changes in the reaction solution were

https://doi.org/10.1021/acsanm.1c00603
ACS Appl. Nano Mater. 2021, 4, 5198−5210

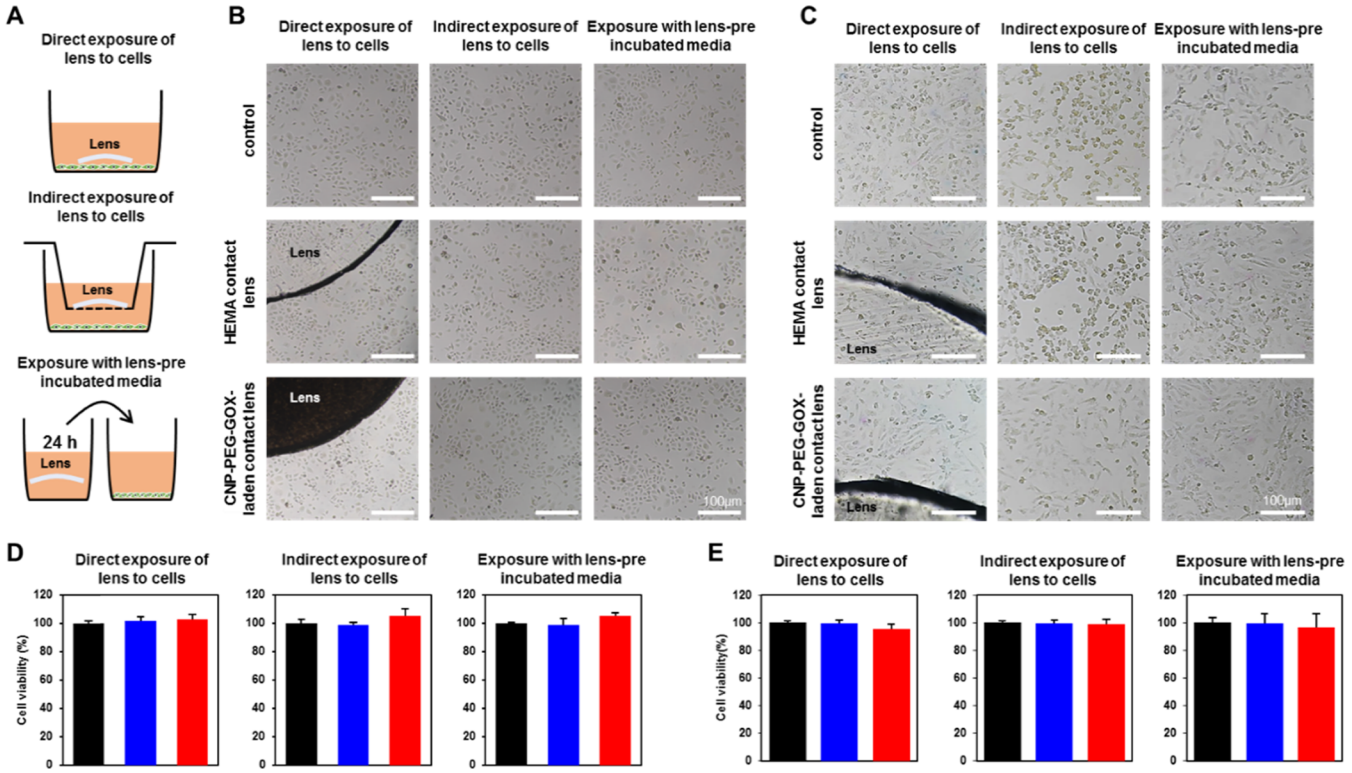

Figure 5. Cytotoxicity of the CNP-PEG-GOx-laden contact lenses on human corneal epithelial cells (HCECs) and human umbilical vein endothelial cells (HUVECs). (A) Schematic diagram of the experiment: (i) Direct treatment of the CNP-PEG-GOx-laden contact lenses to cells; (ii) co-incubation of the CNP-PEG-GOx-laden contact lenses and cells using inserted transwell; (iii) treatment with medium preincubated with the CNP-PEG-GOx-laden contact lens for 24 h. (B) HCEC images from experiments with control, HEMA contact lenses, and CNP-PEG-GOx-laden contact lenses. (C) HUVEC images from experiments with control, HEMA contact lenses, and CNP-PEG-GOx-laden contact lenses. (D) Viability of HCECs in experiments with control (black bar), HEMA contact lenses (blue bar), and CNP-PEG-GOX-laden contact lenses (red bar). Data are presented as the mean ± SEM (n = 5). (E) Viability of HUVECs in experiments with control (black bar), HEMA contact lenses (blue bar), and CNP-PEG-GOx-laden contact lenses (red bar). Data are presented as the mean ± SEM (n = 5).

evaluated at pH 5 and 7 because the normal pH range of human tears is 6.5−7.6.[50] Fortunately, the pH value of the reaction solution did not change in either pH condition during the color development of the CNP-PEG-GOx-laden contact lenses (Figure S19).

To improve visibility through the CNP-PEG-GOx-laden contact lenses, center-transparent contact lenses with CNP-PEG-GOx loaded only at the edges were designed (Figure 4H, inset photograph). It reacted with glucose and changed the color, but the reaction time increased with the increase in thickness (Figure 4H). In addition, it was confirmed that the increase of the thickness does not maintain proper lens characteristics (Figure 4I). It is expected that the problems would be solved through factory-level production later.

2.4. Cytotoxicity of the CNP-PEG-GOx-Laden Contact Lenses to Human Corneal Epithelial Cells (HCECs) and Human Umbilical Vein Endothelial Cells (HUVECs). Next, we evaluated the cytotoxicity of CNP-PEG-GOx. The half-maximal inhibitory concentration (IC_{50}) of CNP-PEG-GOx was ∼1.9 g/L after 24 h of treatment (Figure S20). In previous cytotoxic studies, the IC_{50} values of CNPs on A549 (adenocarcinomic human alveolar basal epithelial cells), HCT-116 cells (human colon cancer cell line), and HaCaT cells (human skin keratinocyte) were 45.5 μg/L, 58.2 μg/L, and 84.1 mg/L, respectively.[51,52] Therefore, our chemical conjugation of CNP dramatically reduced its cytotoxicity. We next tested the cytotoxicity of the CNP-PEG-GOx-laden contact lenses on HCECs and HUVECs because the lenses would be worn in direct contact with the cornea of the eye, and CNP-PEG-GOx released from the lenses might be absorbed into blood vessels and exhibit toxicity (Figure 5A). Fortunately, the CNP-PEG-GOx-laden contact lenses showed no cytotoxicity to HCECs and HUVECs after 24 h of exposure (Figure 5B−E). This result demonstrated that the entrapped CNP-PEG-GOx was not released from the contact lenses, as strongly supported in Figure S15B. The HEMA contact lenses made without nanoparticles also showed no cytotoxicity, indicating that no problems occurred during the fabrication of the contact lenses. Therefore, when the CNP-PEG-GOx-laden contact lenses are worn on the eye, they should cause no toxicity to the cornea because of the stability of the conjugate.

2.5. Ability of the CNP-PEG-GOx-Laden Contact Lenses to Detect Diabetic Rabbits. To confirm the feasibility of using our CNP-PEG-GOx-laden contact lenses in diabetic animals, we tested them on a transient diabetic rabbit model. While a rabbit's blood glucose level was elevated by a glucose injection (4 g/(kg h)), the CNP-PEG-GOx-laden contact lenses were placed on the rabbit's eyes for 30 min, and the normalized b color profile was measured. After that, new CNP-PEG-GOx-laden contact lenses were inserted every 30 min, and the color profile was measured at every change. First of all, we confirmed that the rabbits' blood glucose levels were significantly elevated after the glucose injection (Figure 6A). We observed a color reaction in the CNP-PEG-GOx-laden contact lenses worn by the diabetic rabbits (Figure 6B). The color development of the CNP-PEG-GOx-laden contact lenses

https://doi.org/10.1021/acsanm.1c00603
ACS Appl. Nano Mater. 2021, 4, 5198−5210

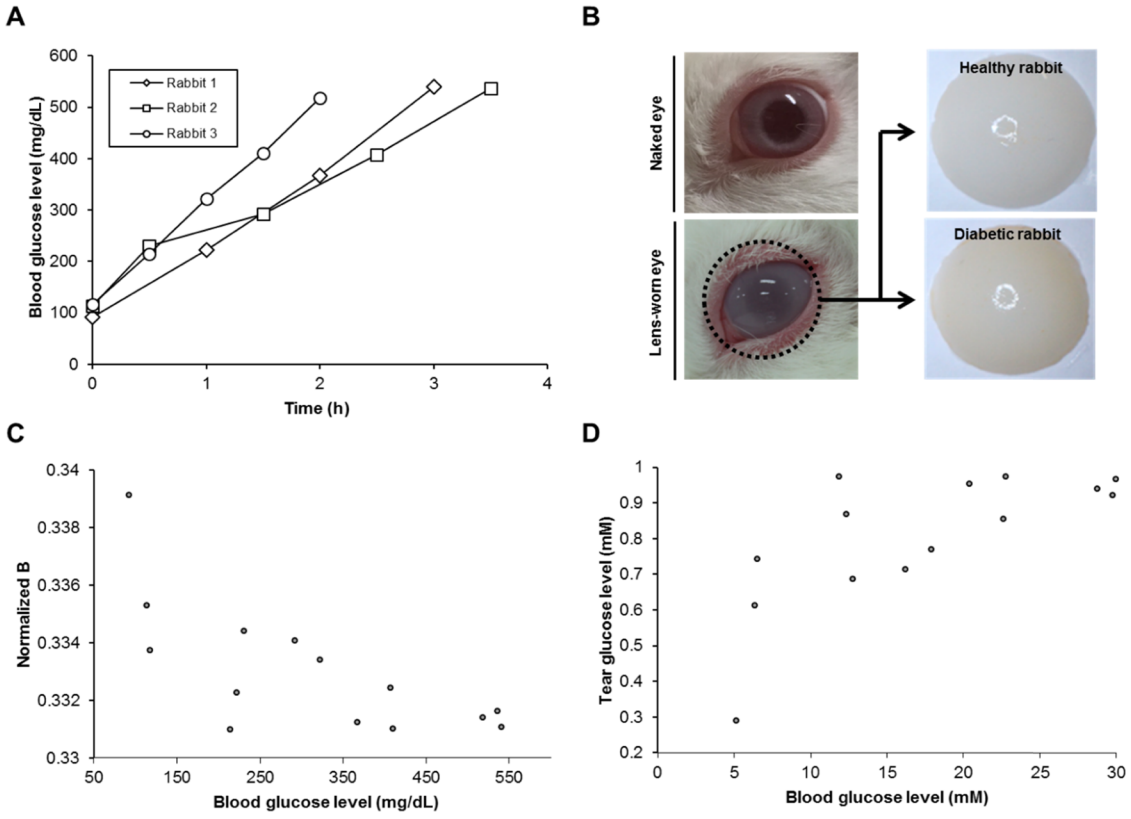

Figure 6. Noninvasive monitoring of tear glucose level in diabetic rabbits wearing the colorimetric CNP-PEG-GOx-laden contact lenses. (A) Invasive, hourly monitoring of blood glucose levels in transiently diabetic rabbits after glucose (4 g/(kg h)) injection (n = 3). (B) Images of the CNP-PEG-GOx-laden contact lenses (930 μg/lens) worn on the eyes of healthy or diabetic rabbits. (C) Inverse proportional correlation between the blood glucose level and the normalized b color profile from the CNP-PEG-GOx-laden contact lenses. (D) Proportional correlation between blood glucose and tear glucose levels.

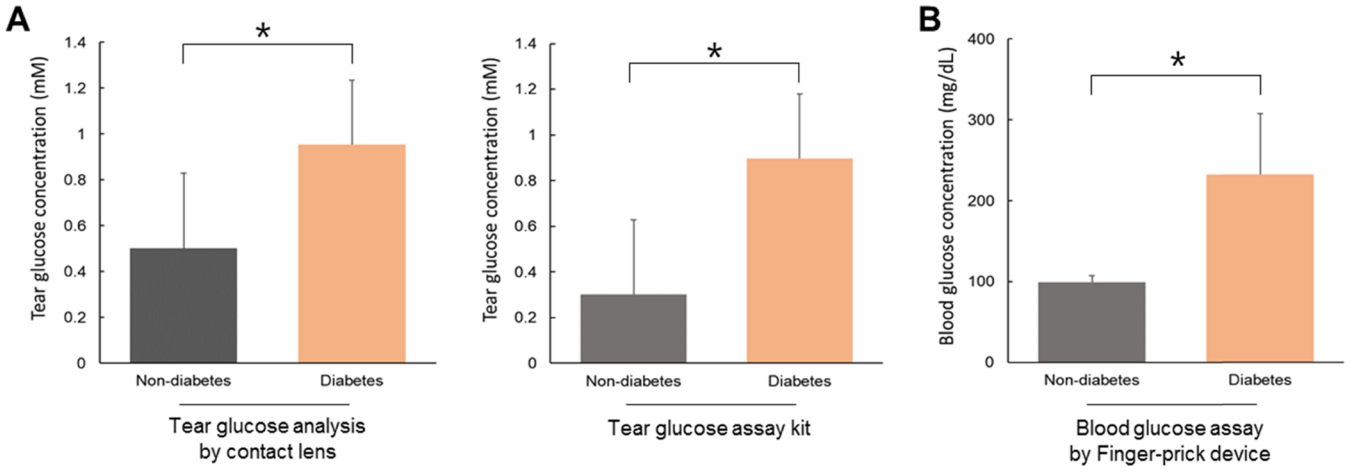

Figure 7. Application of colorimetric CNP-PEG-GOx-laden contact lenses using a portable RGB analysis system to measure glucose in tear specimens from human volunteers. (A) Tear glucose levels of human volunteers analyzed using the CNP-PEG-GOx-laden contact lenses and a glucose assay kit. Data are presented as the mean ± SEM (nondiabetes volunteers: n = 5, diabetes volunteers: n = 5). *P < 0.05. (B) Blood glucose levels of human volunteers analyzed by the finger-prick test with a portable blood glucometer. Data are presented as the mean ± SEM (nondiabetes volunteers: n = 5, diabetes volunteers: n = 5). *P < 0.05.

occurred gradually, with a reduction in the normalized b color profile whenever the blood glucose increased (Figure 6C). The concentration of tear glucose indicated by the normalized b color profile of the CNP-PEG-GOx-laden contact lenses was quantified and plotted together with the blood glucose levels of the rabbits (Figure 6D). That result showed a proportional correlation between the measured tear glucose and blood glucose. In particular, when the blood glucose level increased above the diabetes criterion (~12 mM), the tear glucose level increased rapidly. Collectively, these findings demonstrate the ability of the colorimetric CNP-PEG-GOx-laden contact lenses to noninvasively and reliably monitor the concentration of tear glucose, which can be used to predict blood glucose levels.

https://doi.org/10.1021/acsanm.1c00603
ACS Appl. Nano Mater. 2021, 4, 5198−5210

Table 1. Noninvasive Prediction of Diabetes Mellitus in Human Volunteers According to the Colorimetric Analysis of Tear Specimens Using CNP-PEG-GOx-Laden Contact Lenses

volunteer no.	status	sex	age	blood glucose (mg/dL)	tear glucose by lens (mM)	noninvasive prediction[a]
1	healthy	female	56	101	0.11	normoglycemia
2	healthy	female	28	96	0.35	normoglycemia
3	healthy	male	33	95	0.80	hyperglycemia[d]
4	healthy	male	33	88	0.44	normoglycemia
5	healthy	male	33	117[b]	0.77	hyperglycemia[c]
6	diabetic	female	49	304	1.01	hyperglycemia
7	diabetic	female	58	244	0.66	hyperglycemia
8	diabetic	male	44	119	0.65	hyperglycemia
9	diabetic	female	59	299	1.05	hyperglycemia
10	diabetic	male	59	159	0.84	hyperglycemia

[a]Blind specimen test was carried out by two researchers in each institute. [b]Blood glucose was relatively high at the time of sampling, although the physician judged the volunteer to be healthy. [c]Contact lens predicted hyperglycemia because blood glucose was relatively high at the time of sampling. [d]Contact lens predicted hyperglycemia although the volunteer was healthy.

2.6. Reliability of CNP-PEG-GOx-Laden Contact Lenses with Human Tear Specimens. Next, we evaluated the reliability of the CNP-PEG-GOx-laden contact lenses using tear specimens from human volunteers. Tear specimens were collected from 10 volunteers (5 diabetic patients and 5 healthy persons) using capillary tubes. The collected volume of each tear specimen was 5−10 μL, which was insufficient to wet an entire contact lens (18−21 mm in diameter). Therefore, to analyze the tiny volume of our tear specimens, we fabricated smaller CNP-PEG-GOx-laden contact lenses (approximately 3 mm in diameter). Furthermore, we needed to improve our image acquisition system and calculation algorithm to accommodate the smaller contact lens before and after incubation with glucose. We configured the image acquisition system using a zoom lens and color CCD to analyze the general RGB profile on colorimetric CNP-PEG-GOx-laden contact lenses wet with tear specimens. After that, the central area (0.5 mm^2) of each acquired image was cropped and analyzed using an intensity normalization process (Figure S21). To further normalize the normalized *rgb* color profile on the small colorimetric CNP-PEG-GOx-laden contact lenses, the difference value was calculated before and after incubation with the tear specimens (Figure S22). When glucose samples were incubated with the small CNP-PEG-GOx-laden contact lenses, the difference value of the normalized b (Δb) was used to monitor the different glucose concentrations (Table S2). These results indicate that our small-volume tear specimens were adequately monitored using our small CNP-PEG-GOx-laden contact lenses.

Finally, we measured the tear glucose concentrations in specimens from diabetic and nondiabetic human volunteers using the CNP-PEG-GOx-laden contact lenses and a glucose assay kit (Figure 7A). As measured using the CNP-PEG-GOx-laden contact lenses, the tear glucose concentrations from diabetic and nondiabetic volunteers were 1.0 ± 0.1 and 0.5 ± 0.1 mM, respectively. As measured by the glucose assay kit, the tear glucose concentrations from diabetic and nondiabetic volunteers were 0.90 ± 0.17 and 0.30 ± 0.06 mM, respectively. To confirm the pattern of the tear glucose concentration from diabetic and nondiabetic volunteers, their blood glucose concentrations were measured using the general finger-prick method (Figure 7B). The blood glucose concentrations from diabetic and nondiabetic volunteers were 232.3 ± 26.5 and 99.1 ± 3.4 mg/dL, respectively. Noninvasive prediction of diabetes mellitus in the human volunteers was carried out by analyzing the results from the contact lenses (Table 1) while completely blinded to the conditions of the volunteers. As a result, the status (diabetes or healthy) of the human volunteers was well predicted, except for volunteer no. 3. Also, the tear glucose level in volunteer no. 5 was judged to be from a nondiabetic person, though it was higher than the normal level (<0.6 mM), in accordance with a high blood glucose level at the time of tear collection.

3. CONCLUSIONS

In this research, we developed wearable colorimetric contact lens biosensors using CNPs. To quantitatively analyze the color intensity of the CNP-PEG-GOx-laden contact lenses, we newly invented a smartphone-based normalization algorithm to use the camera module on a smartphone. Using the wearable colorimetric CNP-PEG-GOx-laden contact lenses and normalization color profile algorithm, we noninvasively monitored tear glucose levels and predicted the blood glucose levels of diabetic and healthy human volunteers with good success. For the clinical trial, we will continue the fabrication of GMP (good manufacturing practices)-grade contact lenses loaded with the CNP-PEG-GOx nanocomplex and study our compensation algorithm using a deep-learning application to ensure that it can accommodate various environments, such as indoor/outdoor, sunny/cloudy weather, and hot/cold temperature.

4. EXPERIMENTAL SECTION

4.1. Materials. Ammonium hydroxide (NH_4OH), cerium(III) nitrate hexahydrate ($Ce(NO_3)_3{\cdot}6H_2O$), epichlorohydrin, EDC (1-ethyl-3-(3-dimethylaminopropyl) carbodiimide hydrochloride), NHS (*N*-hydroxysuccinimide), ethylene glycol dimethacrylate (EGDMA), fructose, galactose, glucose, GOx, HEMA, 2-hydroxy-2-methylpropiophenone (photoinitiator), hydrogen peroxide (H_2O_2), methacrylic acid (MAA), sodium chloride (NaCl), sodium hydroxide (NaOH), sucrose, and glucose assay kits (MAK263) were purchased from Sigma-Aldrich (St. Louis, MO). NHS−poly(ethylene glycol)−COOH (M_w 2 kDa) was purchased from Nanocs (New York, NY). Ultrapure deionized water was produced using a Milli-Q system (Millipore, Billerica, MA). Image processing and visualization were performed using Matlab (Mathworks, Natick, MA) and the Open Source Computer Vision Library (OpenCV) (Intel Corporation, Santa Clara).

4.2. Cell Lines and Animals. HUVECs were purchased from Lonza (Basel, Switzerland). HUVEC cultures were kept in endothelial growth medium (EGM-2 bullet kit; Lonza, Basel, Switzerland) containing 10% fetal bovine serum (GenDEPOT, Barker, TX) and 1%

https://doi.org/10.1021/acsanm.1c00603
ACS Appl. Nano Mater. 2021, 4, 5198−5210

antibiotics. HCECs were purchased from ATCC (Manassas, VA). Cell cultures were kept under standard culture conditions of 37 °C and 5% CO_2. The growth medium was changed from 16 to 24 h after seeding and then every other day (every 48 h) thereafter.

Male New Zealand white rabbits (KOATECH, Seoul, Korea) aged 6 months (3.0−4.5 kg) were used in this study. The rabbits were housed in specific pathogen-free conditions in accordance with the provisions of the Institutional Animal Care and Use Committee (IACUC) at Hanyang University. The rabbits were allowed to acclimatize for 7 days before the experiment. Feed was given once a day, and an automated watering system was used. The experimental protocol was approved by the IACUC (No. 2016-0079A) and conformed to the guidelines for the Care and Use of Laboratory Animals.

4.3. Color Space Analysis. Different color models were used to estimate variations in the color profile. Three representative color spaces, CIE *Yxy* (1931), CIELAB (1976) (luminance (*Y*, *L**)), and chroma (*x*, *y*, *a**, and *b**), were compared with the RGB model. CIE *Yxy* (1931) and CIELAB (1976), standardized by the CIE (Commission Internationale de l'Eclairage), are perceptually uniform color spaces independent of brightness.[53] The correlation coefficient (R^2) was calculated through linear regression analyses of the color change at different concentrations of glucose.

4.4. Smartphone-Based Algorithm Interface with Normalization Process for RGB Color. A smartphone-based algorithm interface was proposed for image extraction from the colorimetric CNP-PEG-GOx-laden contact lenses after reaction (Figure S11). We created a grayscale mask image of the region of interest. The 3D RGB color profile was converted into a one-dimensional grayscale to simplify the complexity of the color profile. To recognize the shape of the contact lens, we detected the edge of the sample image in the grayscale by approximating the isotropic gradient based on the Sobel operator.[54,55] After identifying the edge of the lens image, we set the inner and outer areas of the lens image to 1 and 0, respectively, to obtain the mask image in binary form. By compositing the mask image with the color image of the contact lens, we eliminated the shadow and background noise outside the contact lens image, producing a 2D general RGB color profile in the spatial domain for the contact lens image. An intensity normalization process was performed to suppress variations in the illumination and obtain the 2D normalized *rgb* color profile in the spatial domain. During the threshold limitation procedure, glare and other residual noises were set to 0 to make them black, and then the image reconstruction removed all of the black. In the color value detection step, the averaged normalized *rgb* color profile for the contact lens image was obtained by considering the size and number of pixels in the detector. Finally, we evaluated the concentrations of glucose that corresponded with each averaged normalized *rgb* color profile. The normalization equations were

$$\text{normalized } r = \mathrm{R}/(\mathrm{R} + \mathrm{G} + \mathrm{B})$$

$$\text{normalized } g = \mathrm{G}/(\mathrm{R} + \mathrm{G} + \mathrm{B})$$

$$\text{normalized } b = \mathrm{B}/(\mathrm{R} + \mathrm{G} + \mathrm{B})\ (0 \leq r, g, b \leq 1)$$

where RGB was the pixel value of the RGB color profile (0 pixel ≤ R, G, B ≤ 255 pixel).

For self-diagnostic use of this algorithm, the algorithm app developed from the flow chart was ported to Android using Android Developer Tools in Java and OpenCV in C^{++}. The app interface was classified as a "capture and analysis image." The app showed the measured general RGB color profile, normalized *rgb* color profile, and tear glucose concentration from captured or prerecorded images. The concentration gauge for tear glucose was constructed as a function of the extracted normalized *b* color profile and the glucose concentration of the sample. Therefore, a user could easily access both glucose concentration and risk using this gauge. For the operating tests, the app was installed on a Samsung Galaxy $S9^+$ device running Android version 8.0.0 (Movie S1).

4.5. Preparation of CNPs. CNP synthesis was based on the method in a previously published article.[40] Briefly, 1.736 g of cerium(III) nitrate hexahydrate and 400 mg of NaOH were added to 128 mL of distilled water and stirred for 48 h. This solution was washed with distilled water to remove salts. The sample was dried in an oven at 60 °C to obtain CNP powder. High-resolution transmission electron microscopy (HR-TEM) (JEOL JEM-3010) characterized the size and structure of the CNPs. The mean size and size distribution of the CNPs were further determined by dynamic light scattering (DLS) (Malvern Zetasizer Nano ZS). The structure of the CNPs was further observed by X-ray diffraction (Rigaku D/MAX 2500). XPS (VG ESCALAB 220i) was used to explore the atomic composition of the CNPs.

4.6. Color Development of CNPs to Detect H_2O_2 and Glucose. To evaluate whether the CNPs could develop yellow color, the dispersed CNP solution was reacted with various concentrations of H_2O_2 (0, 0.1, 0.2, 0.4, and 0.6 mM) or glucose (0, 0.1, 0.2, 0.4, and 0.6 mM) in the presence of free GOx (100 U/mL) in 96-well plates for 2 min.

4.7. Preparation of CNPs and CNP-PEG-GOx. To modify their surfaces, the synthesized CNPs were dissolved in 1 M NaOH solution, and then epichlorohydrin and NaOH were added and stirred for 8 h. After stirring, the solution was washed with distilled water, and 30% NH_4OH was added and stirred for an additional 14 h. Through this process, the hydroxyl groups of the CNPs were modified to amine groups (CNP-NH_2; M_w 150 kDa). CNP-NH_2 and NHS−PEG−COOH (molar ratio = 1:0.25) were mixed with MES (2-(*N*-morpholino) ethane sulfonic acid) buffer and stirred for 1 h, and this was followed by PEGylation of the CNPs (CNP-PEG). XPS (VG ESCALAB 220i) was used to explore the atomic composition and amination of the CNP-PEG.

To conjugate the CNP-PEG with GOx, EDC and NHS were added to 1 mg/mL of CNP-PEG dissolved in MES buffer, and then the solution was stirred for 20 min. After the pH of the solution was increased to 7.4, GOx was added and stirred for an additional 1 h. The resulting solution was washed with distilled water, producing the CNP-PEG-GOx nanocomplex. To confirm the conjugation of GOx to the CNP-PEG, a UV−vis spectra (Molecular Devices SpectraMax M2) analysis (peak interval: 5 nm wavelength; water solvent: blank) and Bradford protein assay were conducted. SDS-PAGE was performed to elucidate the purity of the CNP-PEG-GOx nanocomplex. The gel used for SDS-PAGE was an 8% acrylamide solution, and it was stained with Coomassie Brilliant Blue.

4.8. Color Development of the CNP-PEG-GOx Nanocomplex to Selectively Detect Glucose. To evaluate whether the GOx-conjugated CNPs could still develop their characteristic yellow color, dispersed CNP-PEG-GOx solution (1 w/v%) was reacted with various concentrations of glucose (0, 0.1, 0.2, 0.4, and 0.6 mM) in 96-well plates for 2 min. To check the responsiveness of the CNP-PEG-GOx nanocomplex against glucose, the color generation of CNP-PEG-GOx was rapidly analyzed as a normalized *b* color profile for each glucose concentration. To elucidate the selectivity of the CNP-PEG-GOx nanocomplex against glucose, the CNP-PEG-GOx solution was reacted with 5 mM of galactose (Gal), glucose (Glu), fructose (Fru), and sucrose (Suc) in 96-well plates for 2 min.

4.9. Fabrication of CNP-PEG-GOx-Laden Contact Lenses. To fabricate the CNP-PEG-GOx-laden contact lenses, HEMA (4 mL) was mixed with 105 μL of MAA and 34 μL of EGDMA, and then 17 μL of photoinitiator was added. Then, different amounts of the CNP-PEG-GOx complex were added to the HEMA-based contact lens solution, which was sufficiently sonicated to disperse CNP-PEG-GOx. After that, the sonicated solution was poured into contact lens molds to fabricate the shape, and then the molds were exposed to UV light (15 mW/cm^2 of intensity at 365 nm) for 30 min to initiate polymerization. The fabricated contact lenses were sufficiently washed with distilled water for 2 days, producing the CNP-PEG-GOx-laden contact lenses. The contact lenses were stored in 0.9% NaCl at 4 °C until use.

To check the light transmittance through the CNP-PEG-GOx-laden contact lenses, the transparency was detected with different

https://doi.org/10.1021/acsanm.1c00603
ACS Appl. Nano Mater. 2021, 4, 5198−5210

amounts (0, 115, 220, 465, and 930 μg/lens) of CNP-PEG-GOx. Because the CNP-PEG-GOx nanocomplex was entrapped in the contact lens, the transmittance of light decreased, which could disrupt the main function of the contact lenses, visual correction. Therefore, to improve the transmittance of light, a hybrid contact lens manufacturing method was applied so that the central part of the contact lens was free from the nanocomplex to allow sufficient light transmittance, and the nanocomplexes were placed at the edges of the contact lenses for color development upon exposure to tear glucose (Figure 4H).

To predict the wearing comfort, the elastic modulus and wettability of the CNP-PEG-GOx-laden contact lenses were measured. A rotational rheometer (Malvern Gemini HRnano Rotational Rheometer; Bohlin Gemini 150; Malvern Panalytical Ltd, Malvern, United Kingdom) was used to measure the elastic modulus of the CNP-PEG-GOx-laden contact lenses. The elastic modulus was recorded at 0.5% strain, 0.05−100 Hz, and 25 °C. To evaluate the wettability of the CNP-PEG-GOx-laden contact lenses, the diameter and height of the lenses were measured before and after hydration. In addition, the EWC was calculated for each group of contact lenses. The EWC equation is as follows

$$\mathrm{EWC} = (W_s - W_d)/W_s$$

W_s is the mass of the swollen contact lens (after hydration) and W_d is the mass of the dry contact lens (before hydration)

4.10. Color Development of CNP-PEG-GOx-Laden Contact Lenses to Monitor Low Glucose Concentrations in Saline and Artificial Tears. To evaluate whether the CNP-PEG-GOx-laden contact lenses could develop the characteristic yellow color, lenses containing various amounts (0, 115, 220, 465, and 930 μg/lens) of CNP-PEG-GOx were reacted with glucose solution (0.6 mM) for different reaction times (0, 10, 30, and 60 min). To compare the reactivity of the CNP-PEG-GOx-laden contact lenses in different solutions, the CNP-PEG-GOx-laden lenses (930 μg/lens) were reacted with glucose (0, 0.2, 0.4, 0.6, and 1.2 mM) in saline buffer (0.9% NaCl solution) and artificial tears (Eyemiru, CJ Healthcare, Korea).

Color development in the CNP-PEG-GOx-laden contact lenses might be affected by pH because of the enzymatic reaction of GOx. In general, the normal pH range for human tears is 6.5−7.5, for a mean value of about 7.0.[50] The pH range for optimal GOx activity is 4−7, for a mean value of about 5.5.[56] Therefore, to evaluate whether the color development of the CNP-PEG-GOx-laden contact lenses would be affected, the reaction was run under different pH conditions (pH 5 or 7), and changes in the pH value during the reaction were also measured.

4.11. Cytotoxicity of CNP-PEG-GOx-Laden Contact Lenses to HCECs and HUVECs. The cytotoxicity of the CNP-PEG-GOx nanocomplex itself was measured in HUVECs (1×10^4 cells/well in 96-well plates) using a Cell Counting Kit-8 (CCK; Dojindo, Japan). Briefly, the HUVECs seeded in the plates were incubated for 24 h in an incubator (at 37 °C, 5% CO_2) and then treated with various concentrations (0, 0.5, 1, 5, 10, 20, 50, 100, 200, 500, 1000, 2000, 4000, and 6000 μg/mL) of CNP-PEG-GOx for 24 h. After treatment, the medium was removed and CCK (10% of medium volume) was administered to the HUVECs and incubated for 2 h. The absorbance at 450 nm was measured using a microplate reader.

Next, to evaluate whether the CNP-PEG-GOx-laden contact lenses could damage the cornea, the viability of HCECs and HUVECs against CNP-PEG-GOx-laden contact lenses (3 mm in diameter) was measured for 24 h. To clearly evaluate the cytotoxicity, HCECs and HUVECs (6×10^4 cells/well in 24-well plates) were incubated in three experimental conditions: direct exposure of cells to the lens, indirect exposure of cells to the lens, and exposure of the cells to medium preincubated with the lens (Figure 5A). After 24 h of incubation, the CNP-PEG-GOx-laden contact lens was carefully removed, and CCK (10% of medium volume) was administered to the cells for 2 h. Absorbance at 450 nm was measured using a microplate reader.

4.12. Noninvasive Monitoring of Tear Glucose Levels in Hyperglycemic Rabbits Wearing the Colorimetric CNP-PEG-GOx-Laden Contact Lenses. Modeling diabetes in rabbits using streptozotocin (STZ) is difficult. STZ is highly toxic in rabbits, resulting in a high mortality rate. Therefore, we created a transient hyperglycemic rabbit model.

To transiently induce hyperglycemia in rabbits, male New Zealand white rabbits (Koatech, Seoul, Korea) aged 6 months (3.0−4.5 kg body weight) were subcutaneously injected with a high concentration of glucose (4 g/kg) every hour until the blood glucose level was above 500 mg/dL. To evaluate whether the CNP-PEG-GOx-laden contact lenses could noninvasively monitor tear glucose levels, CNP-PEG-GOx-laden contact lenses were placed on the eyes of the hyperglycemic rabbits for 30 min. For comparison with the tear glucose level, blood was taken from the ear veins of each rabbit with a lancet, and the blood glucose level was measured using a portable glucometer (ACCU-CHEK, Roche Diagnostics, Basel, Switzerland).

4.13. Collection of Tear Specimens from Healthy and Diabetic Human Volunteers. To test the ability of the CNP-PEG-GOx-laden contact lenses to noninvasively monitor tear glucose, human tear specimens were taken from diabetic and nondiabetic volunteers. All human research was approved by the Institutional Review Board (IRB) of Hanyang University (IRB No. HYI-18-182-1) and the IRB of Kyung Hee University Hospital at Gangdong (No. KHNMC2018-07-009-001) and adhered to the tenets of the Declaration of Helsinki for human research. Written informed consent was obtained from all volunteers. Tear specimens were collected from 10 participants (5 diabetes patients and 5 healthy persons) using capillary tubes. Diabetes mellitus was diagnosed according to the criteria of the Korean Diabetes Association clinical practice guideline.[57] Before the tears were collected, venous blood specimens were collected for blood glucose analysis. The blood glucose levels were measured using an enzymatic UV method (AU5800; Beckman Coulter Inc., Brea, CA). The blood glucose concentration of each subject was blinded to all of the researchers in each institute who measured tear glucose levels using the colorimetric CNP-PEG-GOx-laden contact lenses.

Tear collection was performed by placing the tip of a capillary tube on the conjunctival sac and the lateral canthus under slit-lamp microscopy. The collection time was a maximum of 5 min, and the collection volumes were between 5 and 10 μL. During tear collection, care was taken to avoid touching either the cornea or conjunctiva to minimize reflex lacrimation. The collected tears were expelled from the capillary tubes into 0.1 mL Eppendorf PCR tubes (Eppendorf reaction tube; Eppendorf−Netheler−Hinz GmbH, Hamburg, Germany) using a micropipette. All collected tear specimens were stored at −70 °C until colorimetric analysis with the CNP-PEG-GOx-laden contact lenses.

4.14. Configuration of Portable RGB Analysis System for Small CNP-PEG-GOx-Laden Contact Lenses to Accommodate the Tiny Volume of the Human Tear Specimens. The volume of the collected tear specimens was 5−10 μL, which was insufficient to wet an entire contact lens (18−21 mm in diameter). Therefore, to analyze the glucose levels in the tiny tear specimens, we fabricated smaller CNP-PEG-GOx-laden contact lenses (approximately 3 mm in diameter). This meant that we needed to improve the image acquisition system to fit the smaller contact lens before and after incubation with glucose (Figure S22).

4.15. Monitoring Glucose Levels in Human Tear Specimens Using the CNP-PEG-GOx-Laden Contact Lenses. To monitor the glucose levels in the human tear specimens, we captured an image of the small CNP-PEG-GOx-laden contact lenses to measure their RGB color variation before incubation with the human tear specimens. After that, we placed a human tear (5 μL) on the contact lens for 30 min and then captured an image of the contact lens to measure the RGB color variation. To analyze the general RGB color profile, we cropped the region of interest to 50 × 50 pixels on the central area (0.5 mm^2) of the contact lens before and after incubation (Figure S21). Then, we calculated the difference value of the normalized *rgb*

https://doi.org/10.1021/acsanm.1c00603
ACS Appl. Nano Mater. 2021, 4, 5198−5210

color profile of the lenses exposed to a human tear specimen using the following modified normalization algorithm (Figure S22)

$$\Delta\text{normalized } r = R^A/(R^A + G^A + B^A) - R^B/(R^B + G^B + B^B)$$

$$\Delta\text{normalized } g = G^A/(R^A + G^A + B^A) - G^B/(R^B + G^B + B^B)$$

$$\Delta\text{normalized } b = B^A/(R^A + G^A + B^A) - B^B/(R^B + G^B + B^B)$$

where R^B, G^B, and B^B are the pixel values of the RGB color profile before incubation with the tear specimen and R^A, G^A, and B^A are the pixel values of the RGB color profile after incubation with the tear specimen (0 pixel ≤ R, G, B ≤ 255 pixel).

The difference value of the normalized *rgb* color profile was converted to the concentration of tear glucose using the standard curve equation. Finally, the glucose concentration in each human tear specimen was converted into a blood glucose concentration using Dawn and Hill's correlation coefficient between blood glucose and tear glucose.[58] To confirm the reliability of the CNP-PEG-GOx-laden contact lenses, we separately measured the glucose levels in the same tear specimens using a glucose assay kit (MAK263-1KT, Sigma-Aldrich, St. Louis).

4.16. Statistics. All data are presented as the mean ± SEM. Statistical analysis of the data was performed using *t*-testing in Systat software to compare the test groups with the control groups. $P < 0.05$ was considered significant.

■ ASSOCIATED CONTENT

Supporting Information

The Supporting Information is available free of charge at https://pubs.acs.org/doi/10.1021/acsanm.1c00603.

XPS spectra of O 1s and Ce 3d for CNPs; normalization equation for RGB color analysis; linear regression graph between hydrogen peroxide (H_2O_2) and normalized *b* values at various concentrations of CNPs; linear regression graph between glucose and normalized *b* values at various concentrations of CNPs; schematic illustration of the chemical conjugation of PEG and an aminated CNP nanoparticle; analysis of surface-modified CNPs; schematic illustration of the synthesis of the CNP-PEG-GOx conjugate; UV−vis absorbance spectra for GOx, CNP-PEG, and CNP-PEG-GOx; SDS-PAGE of free GOx alone and a mixture of GOx with CNP-PEG-GOx; linear regression graph between glucose and normalized *b* values at various concentrations of CNP-PEG-GOx; flow charts for the glucose colorimetric detection algorithm; intensity normalization process; process used by the smartphone app to measure the general RGB color profile, normalized *rgb* color profile, and calculated value for tear glucose concentration; scanning electron microscope image of HEMA lens without any CNP or GOx, CNP-PEG-GOx-laden contact lens, and CNP/GOx mixture-laden contact lens; stability of CNP-PEG-GOX-laden contact lens; yellow color development of CNP-PEG-GOx-laden contact lenses and CNP/GOx mixture-laden contact lenses after reaction with 2 mL of glucose solution for 10 min; reliability of CNP-PEG-GOx-laden contact lenses; color images of CNP-PEG-GOX-laden contact lenses at each reaction time after treatment with various concentrations of glucose in buffer or artificial tear solution; changes in the normalized pH value during color development of CNP-PEG-GOx-laden contact lenses exposed to glucose solution; cytotoxicity of CNP-PEG-GOX to human umbilical vein endothelial cells; general RGB images and normalized *rgb* images of small CNP-PEG-GOx-laden contact lenses after cropping the central area on the acquired images; calculation of the difference value of the normalized *rgb* color profiles from small CNP-PEG-GOx-laden contact lenses before and after incubation with tear specimens; quantification of the conjugated amount of GOx to the CNP-PEG-GOx nanocomplex; and difference value of normalized *rgb* color profiles on CNP-PEG-GOx-laden contact lens with small size before and after incubation of different glucose concentration (PDF)

Glucose sensing video using the app (Movie S1) (MP4)

■ AUTHOR INFORMATION

Corresponding Author

Dong Yun Lee − *Department of Bioengineering, College of Engineering, and BK FOUR Biopharmaceutical Innovation Leader for Education and Research Group, and Institute of Nano Science & Technology (INST), Hanyang University, Seoul 04763, Republic of Korea;* orcid.org/0000-0001-7691-0447; Phone: +82-2-2220-2348; Email: dongyunlee@hanyang.ac.kr; Fax: +82-2-2220-4741

Authors

Sijin Park − *Department of Bioengineering, College of Engineering, and BK FOUR Biopharmaceutical Innovation Leader for Education and Research Group, and Institute of Nano Science & Technology (INST), Hanyang University, Seoul 04763, Republic of Korea*

Juil Hwang − *Department of Physics, College of Natural Sciences, Hanyang University, Seoul 04763, Republic of Korea*

Hee-Jae Jeon − *Department of Biomedical Engineering, Purdue University, West Lafayette, Indiana 47907-2050, United States; Department of Biomedical Science and Engineering, Gwangju Institute of Science and Technology, Gwangju 61005, Republic of Korea*

Woo Ri Bae − *Department of Bioengineering, College of Engineering, and BK FOUR Biopharmaceutical Innovation Leader for Education and Research Group, and Institute of Nano Science & Technology (INST), Hanyang University, Seoul 04763, Republic of Korea*

In-Kyung Jeong − *Department of Endocrinology and Metabolism, Kyung Hee University Hospital at Gangdong, Kyung Hee University School of Medicine, Seoul 05278, Republic of Korea*

Tae Gi Kim − *Department of Ophthalmology, Kyung Hee University Hospital at Gangdong, Kyung Hee University School of Medicine, Seoul 05278, Republic of Korea*

Jaheon Kang − *Department of Ophthalmology, Kyung Hee University Hospital at Gangdong, Kyung Hee University School of Medicine, Seoul 05278, Republic of Korea*

Young-Geun Han − *Department of Physics, College of Natural Sciences, Hanyang University, Seoul 04763, Republic of Korea*

Euiheon Chung − *Department of Biomedical Science and Engineering, Gwangju Institute of Science and Technology, Gwangju 61005, Republic of Korea*

Complete contact information is available at: https://pubs.acs.org/10.1021/acsanm.1c00603

https://doi.org/10.1021/acsanm.1c00603
ACS Appl. Nano Mater. 2021, 4, 5198−5210

Author Contributions

D.Y.L. fully managed the research effort. S.P. and W.R.B. contributed to the design, development, and analysis of material for the in vitro data. S.P. and D.Y.L. contributed to the design and analysis of the in vivo data. S.P. and D.Y.L. wrote the manuscript with the help of the co-authors. J.H. and Y.-G.H. contributed to the design and development of the colorimetric image-processing algorithm and wrote the relevant part of the manuscript. S.P., H.-J.J., E.C., and D.Y.L. contributed to the design and development of the color analysis system for clinical samples and wrote the relevant part of the manuscript. I.-K.J., T.G.K., and J.K. contributed to the design and processing of the human study, including collecting human tears, and wrote the relevant part of the manuscript.

Notes

The authors declare no competing financial interest.

■ ACKNOWLEDGMENTS

This research was supported by the National Research Foundation of Korea (NRF) funded by the Ministry of Science, ICT & Future Planning (NRF-2015M3A9E2030125 and NRF-2020R1A2C3005834).

■ REFERENCES

(1) Veiseh, O.; Tang, B. C.; Whitehead, K. A.; Anderson, D. G.; Langer, R. Managing diabetes with nanomedicine: challenges and opportunities. *Nat. Rev. Drug Discovery* **2015**, *14*, 45−57.

(2) Ohkubo, Y.; Kishikawa, H.; Araki, E.; Miyata, T.; Isami, S.; Motoyoshi, S.; Kojima, Y.; Furuyoshi, N.; Shichiri, M. Intensive insulin therapy prevents the progression of diabetic microvascular complications in Japanese patients with non-insulin-dependent diabetes mellitus: a randomized prospective 6-year study. *Diabetes Res. Clin. Pract.* **1995**, *28*, 103−117.

(3) Klonoff, D. C.; Buckingham, B.; Christiansen, J. S.; Montori, V. M.; Tamborlane, W. V.; Vigersky, R. A.; Wolpert, H. Continuous glucose monitoring: an Endocrine Society Clinical Practice Guideline. *J. Clin. Endocrinol. Metab.* **2011**, *96*, 2968−2979.

(4) Huang, E. S.; O'Grady, M.; Basu, A.; Winn, A.; John, P.; Lee, J.; Meltzer, D.; Kollman, C.; Laffel, L.; Tamborlane, W.; Weinzimer, S.; Wysocki, T. Juvenile Diabetes Research Foundation Continuous Glucose Monitoring Study, G. The cost-effectiveness of continuous glucose monitoring in type 1 diabetes. *Diabetes Care* **2010**, *33*, 1269−1274.

(5) Juvenile Diabetes Research Foundation Continuous Glucose Monitoring Study, G.. Prolonged nocturnal hypoglycemia is common during 12 months of continuous glucose monitoring in children and adults with type 1 diabetes. *Diabetes Care* **2010**, *33*, 1004−1008.

(6) American Diabetes, A.. 5. Glycemic Targets. *Diabetes Care* **2016**, *39*, S39−S46.

(7) Burge, M. R. Lack of compliance with home blood glucose monitoring predicts hospitalization in diabetes. *Diabetes Care* **2001**, *24*, 1502−1503.

(8) Zhang, J.; Hodge, W.; Hutnick, C.; Wang, X. Noninvasive diagnostic devices for diabetes through measuring tear glucose. *J. Diabetes Sci. Technol.* **2011**, *5*, 166−172.

(9) Farandos, N. M.; Yetisen, A. K.; Monteiro, M. J.; Lowe, C. R.; Yun, S. H. Contact lens sensors in ocular diagnostics. *Adv. Healthcare Mater.* **2015**, *4*, 792−810.

(10) Chu, M. X.; Miyajima, K.; Takahashi, D.; Arakawa, T.; Sano, K.; Sawada, S.; Kudo, H.; Iwasaki, Y.; Akiyoshi, K.; Mochizuki, M.; Mitsubayashi, K. Soft contact lens biosensor for in situ monitoring of tear glucose as non-invasive blood sugar assessment. *Talanta* **2011**, *83*, 960−965.

(11) Lee, H.; Choi, T. K.; Lee, Y. B.; Cho, H. R.; Ghaffari, R.; Wang, L.; Choi, H. J.; Chung, T. D.; Lu, N.; Hyeon, T.; Choi, S. H.; Kim, D. H. A graphene-based electrochemical device with thermoresponsive microneedles for diabetes monitoring and therapy. *Nat. Nanotechnol.* **2016**, *11*, 566−572.

(12) Yao, H.; Shum, A. J.; Cowan, M.; Lahdesmaki, I.; Parviz, B. A. A contact lens with embedded sensor for monitoring tear glucose level. *Biosens. Bioelectron.* **2011**, *26*, 3290−3296.

(13) Kim, S.; Jeon, H. J.; Park, S.; Lee, D. Y.; Chung, E. Tear Glucose Measurement by Reflectance Spectrum of a Nanoparticle Embedded Contact Lens. *Sci. Rep.* **2020**, *10*, No. 8254.

(14) Keum, D. H.; Kim, S. K.; Koo, J.; Lee, G. H.; Jeon, C.; Mok, J. W.; Mun, B. H.; Lee, K. J.; Kamrani, E.; Joo, C. K.; Shin, S.; Sim, J. Y.; Myung, D.; Yun, S. H.; Bao, Z.; Hahn, S. K. Wireless smart contact lens for diabetic diagnosis and therapy. *Sci. Adv.* **2020**, *6*, No. eaba3252.

(15) Park, J.; Kim, J.; Kim, S. Y.; Cheong, W. H.; Jang, J.; Park, Y. G.; Na, K.; Kim, Y. T.; Heo, J. H.; Lee, C. Y.; Lee, J. H.; Bien, F.; Park, J. U. Soft, smart contact lenses with integrations of wireless circuits, glucose sensors, and displays. *Sci. Adv.* **2018**, *4*, No. eaap9841.

(16) Thomas, N.; Lahdesmaki, I.; Parviz, B. A. A contact lens with an integrated lactate sensor. *Sens. Actuators, B* **2012**, *162*, 128−134.

(17) Yao, H.; Liao, Y.; Lingley, A. R.; Afanasiev, A.; Lahdesmaki, I.; Otis, B. P.; Parviz, B. A. A contact lens with integrated telecommunication circuit and sensors for wireless and continuous tear glucose monitoring. *J. Micromech. Microeng.* **2012**, *22*, No. 075007.

(18) Badugu, R.; Lakowicz, J. R.; Geddes, C. D. Noninvasive continuous monitoring of physiological glucose using a monosaccharide-sensing contact lens. *Anal. Chem.* **2004**, *76*, 610−618.

(19) Badugu, R.; Lakowicz, J. R.; Geddes, C. D. A glucose-sensing contact lens: from bench top to patient. *Curr. Opin. Biotechnol.* **2005**, *16*, 100−107.

(20) Elsherif, M.; Hassan, M. U.; Yetisen, A. K.; Butt, H. Wearable Contact Lens Biosensors for Continuous Glucose Monitoring Using Smartphones. *ACS Nano* **2018**, *12*, 5452−5462.

(21) Zhang, C. J.; Cano, G. G.; Braun, P. V. Linear and Fast Hydrogel Glucose Sensor Materials Enabled by Volume Resetting Agents. *Adv. Mater.* **2014**, *26*, 5678−5683.

(22) Ruan, J. L.; Chen, C.; Shen, J. H.; Zhao, X. L.; Qian, S. H.; Zhu, Z. G. A Gelated Colloidal Crystal Attached Lens for Noninvasive Continuous Monitoring of Tear Glucose. *Polymers* **2017**, *9*, No. 125.

(23) Korsvik, C.; Patil, S.; Seal, S.; Self, W. T. Superoxide dismutase mimetic properties exhibited by vacancy engineered ceria nanoparticles. *Chem. Commun.* **2007**, 1056−1058.

(24) Pirmohamed, T.; Dowding, J. M.; Singh, S.; Wasserman, B.; Heckert, E.; Karakoti, A. S.; King, J. E. S.; Seal, S.; Self, W. T. Nanoceria exhibit redox state-dependent catalase mimetic activity. *Chem. Commun.* **2010**, *46*, 2736−2738.

(25) Asati, A.; Santra, S.; Kaittanis, C.; Nath, S.; Perez, J. M. Oxidase-Like Activity of Polymer-Coated Cerium Oxide Nanoparticles. *Angew. Chem., Int. Ed.* **2009**, *48*, 2308−2312.

(26) Hickman, J. J.; Das, M.; Patil, S.; Bhargava, N.; Kang, J. F.; Riedel, L.; Seal, S. Auto-catalytic Ceria nanoparticles offer neuroprotection to adult rat spinal cord neurons. *Tissue Eng.* **2007**, *13*, 873−874.

(27) Kaittanis, C.; Santra, S.; Asati, A.; Perez, J. M. A cerium oxide nanoparticle-based device for the detection of chronic inflammation via optical and magnetic resonance imaging. *Nanoscale* **2012**, *4*, 2117−2123.

(28) Lin, Y.; Xu, C.; Ren, J.; Qu, X. Using thermally regenerable cerium oxide nanoparticles in biocomputing to perform label-free, resettable, and colorimetric logic operations. *Angew. Chem., Int. Ed.* **2012**, *51*, 12579−12583.

(29) Asati, A.; Kaittanis, C.; Santra, S.; Perez, J. M. pH-Tunable Oxidase-Like Activity of Cerium Oxide Nanoparticles Achieving Sensitive Fluorigenic Detection of Cancer Biomarkers at Neutral pH. *Anal. Chem.* **2011**, *83*, 2547−2553.

(30) Kim, M. I.; Park, K. S.; Park, H. G. Ultrafast colorimetric detection of nucleic acids based on the inhibition of the oxidase activity of cerium oxide nanoparticles. *Chem. Commun.* **2014**, *50*, 9577−9580.

https://doi.org/10.1021/acsanm.1c00603
ACS Appl. Nano Mater. 2021, 4, 5198−5210

(31) Njagi, J.; Ispas, C.; Andreescu, S. Mixed ceria-based metal oxides biosensor for operation in oxygen restrictive environments. *Anal. Chem.* **2008**, *80*, 7266−7274.
(32) Lin, Y. H.; Xu, C.; Ren, J. S.; Qu, X. G. Using Thermally Regenerable Cerium Oxide Nanoparticles in Biocomputing to Perform Label-free, Resettable, and Colorimetric Logic Operations. *Angew. Chem., Int. Ed.* **2012**, *51*, 12579−12583.
(33) Ornatska, M.; Sharpe, E.; Andreescu, D.; Andreescu, S. Paper bioassay based on ceria nanoparticles as colorimetric probes. *Anal. Chem.* **2011**, *83*, 4273−4280.
(34) Lang, N. J.; Liu, B. W.; Liu, J. W. Characterization of glucose oxidation by gold nanoparticles using nanoceria. *J. Colloid Interface Sci.* **2014**, *428*, 78−83.
(35) Ozcan, A. Mobile phones democratize and cultivate next-generation imaging, diagnostics and measurement tools. *Lab Chip* **2014**, *14*, 3187−3194.
(36) Wei, Q.; Qi, H.; Luo, W.; Tseng, D.; Ki, S. J.; Wan, Z.; Gorocs, Z.; Bentolila, L. A.; Wu, T. T.; Sun, R.; Ozcan, A. Fluorescent imaging of single nanoparticles and viruses on a smart phone. *ACS Nano* **2013**, *7*, 9147−9155.
(37) Zhu, H.; Sencan, I.; Wong, J.; Dimitrov, S.; Tseng, D.; Nagashima, K.; Ozcan, A. Cost-effective and rapid blood analysis on a cell-phone. *Lab Chip* **2013**, *13*, 1282−1288.
(38) Yetisen, A. K.; Martinez-Hurtado, J. L.; Garcia-Melendrez, A.; Vasconcellos, F. D.; Lowe, C. R. A smartphone algorithm with inter-phone repeatability for the analysis of colorimetric tests. *Sens. Actuators, B* **2014**, *196*, 156−160.
(39) Shen, L.; Hagen, J. A.; Papautsky, I. Point-of-care colorimetric detection with a smartphone. *Lab Chip* **2012**, *12*, 4240−4243.
(40) Chelliah, M.; Rayappan, J. B. B.; Krishnan, U. M. Synthesis and Characterization of Cerium Oxide Nanoparticles by Hydroxide Mediated Approach. *J. Appl. Sci.* **2012**, *12*, 1734−1737.
(41) Abe, K.; Higashi, K.; Watabe, K.; Kobayashi, A.; Limwikrant, W.; Yamamoto, K.; Moribe, K. Effects of the PEG molecular weight of a PEG-lipid and cholesterol on PEG chain flexibility on liposome surfaces. *Colloid Surf., A* **2015**, *474*, 63−70.
(42) Ishii, T.; Miyata, K.; Anraku, Y.; Naito, M.; Yi, Y.; Jinbo, T.; Takae, S.; Fukusato, Y.; Hori, M.; Osada, K.; Kataoka, K. Enhanced target recognition of nanoparticles by cocktail PEGylation with chains of varying lengths. *Chem. Commun.* **2016**, *52*, 1517−1519.
(43) Baca, J. T.; Finegold, D. N.; Asher, S. A. Tear glucose analysis for the noninvasive detection and monitoring of diabetes mellitus. *Ocul. Surf.* **2007**, *5*, 280−293.
(44) Philipp, I.; Rath, T. Improving plant discrimination in image processing by use of different colour space transformations. *Comput. Electron. Agric.* **2002**, *35*, 1−15.
(45) Logan, H. Fundamental aspects of lighting. *Electr. Eng.* **1958**, *77*, 36−41.
(46) Chandra, N.; Khare, K. In *Dictionary Based Approach to Edge Detection*, 2015.
(47) Committee, A. M. Uses (proper and improper) of correlation coefficients. *Analyst* **1988**, *113*, 1469−1471.
(48) Nagelkerke, N. J. A note on a general definition of the coefficient of determination. *Biometrika* **1991**, *78*, 691−692.
(49) Lane, J. D.; Krumholz, D. M.; Sack, R. A.; Morris, C. Tear glucose dynamics in diabetes mellitus. *Curr. Eye Res.* **2006**, *31*, 895−901.
(50) Abelson, M. B.; Udell, I. J.; Weston, J. H. Normal human tear pH by direct measurement. *Arch. Ophthalmol.* **1981**, *99*, No. 301.
(51) Ngoc, L. T. N.; Bui, V. K. H.; Moon, J. Y.; Lee, Y. C. In-Vitro Cytotoxicity and Oxidative Stress Induced by Cerium Aminoclay and Cerium Oxide Nanoparticles in Human Skin Keratinocyte Cells. *J. Nanosci. Nanotechnol.* **2019**, *19*, 6369−6375.
(52) Balaji, S.; Mandal, B. K.; Vinod Kumar Reddy, L.; Sen, D. Biogenic Ceria Nanoparticles (CeO2 NPs) for Effective Photo-catalytic and Cytotoxic Activity. *Bioengineering* **2020**, *7*, No. 26.
(53) Abbott, J. A. Quality measurement of fruits and vegetables. *Postharvest Biol. Technol.* **1999**, *15*, 207−225.
(54) Sobel, I. An Isotropic 3 × 3 Image Gradient Operator. In *Machine Vision for Three-Dimensional Scenes*; Academic Press: London, 1990; pp 376−379.
(55) Gupta, S.; Mazumdar, S. G. Sobel edge detection algorithm. *Int. J. Comput. Sci. Manage. Res.* **2013**, *2*, 1578−1583.
(56) Bright, H. J.; Appleby, M. The pH dependence of the individual steps in the glucose oxidase reaction. *J. Biol. Chem.* **1969**, *244*, 3625−3634.
(57) Kim, M. K.; Ko, S. H.; Kim, B. Y.; Kang, E. S.; Noh, J.; Kim, S. K.; Park, S. O.; Hur, K. Y.; Chon, S.; Moon, M. K.; Kim, N. H.; Kim, S. Y.; Rhee, S. Y.; Lee, K. W.; Kim, J. H.; Rhee, E. J.; Chun, S.; Yu, S. H.; Kim, D. J.; Kwon, H. S.; Park, K. S.; Committee of Clinical Practice Guidelines, K. D. A.. 2019 Clinical Practice Guidelines for Type 2 Diabetes Mellitus in Korea. *Diabetes Metab. J.* **2019**, *43*, 398−406.
(58) Daum, K. M.; Hill, R. M. Human tear glucose. *Invest. Ophthalmol. Visual Sci.* **1982**, *22*, 509−514.

https://doi.org/10.1021/acsanm.1c00603
ACS Appl. Nano Mater. 2021, 4, 5198−5210